JAERI-M
82-054

COMPARISON OF SHIELDING CAPABILITIES OF FUSION REACTOR BLANKET AND SHIELD MATERIALS

June 1982

Yasushi SEKI, Hiromasa IIDA and Hiromitsu KAWASAKI*

日 本 原 子 力 研 究 所
Japan Atomic Energy Research Institute

JAERI-M レポートは，日本原子力研究所が不定期に公刊している研究報告書です。

入手の問合わせは，日本原子力研究所技術情報部情報資料課（〒319—11 茨城県那珂郡東海村）あて，お申しこしください。なお，このほかに財団法人原子力弘済会資料センター（〒319—11 茨城県那珂郡東海村日本原子力研究所内）で複写による実費頒布をおこなっております。

JAERI-M reports are issued irregularly.

Inquiries about availability of the reports should be addressed to Information Section, Division of Technical Information, Japan Atomic Energy Research Institute, Tokai-mura, Naka-gun, Ibaraki-ken 319—11, Japan.

編集兼発行　日本原子力研究所
印　　刷　日立高速印刷株式会社

JAERI-M 82-054

Comparison of Shielding Capabilities of Fusion Reactor Blanket and Shield Materials

Yasushi SEKI, Hiromasa IIDA and Hiromitsu KAWASAKI*

Division of Large Tokamak Development,
Tokai Research Establishment, JAERI

(Received May 12, 1982)

Radiation shielding capabilities of six candidate materials for the blanket and shield of a fusion reactor are compared. The six materials with widely differing nuclear characteristics, namely lead, stainless steel, heavy concrete, ordinary concrete, lithium oxide and water are selected for the comparison. The attenuation of various nuclear quantities and response values in the materials placed in a simplified model of a tokamak fusion reactor is calculated. The result of the calculations are shown graphically and compared in summary tables.

Among the six materials compared, stainless steel, heavy concrete and lead are found to be the best materials for shielding the 14 MeV neutron flux, the total neutron flux and the total gamma ray flux, respectively.

Keywords: Fusion Reactor, Shielding, D-T Neutrons, 14 MeV Neutrons, Gamma Ray, Shield Material, Lead, Stainless Steel, Heavy Concrete, Ordinary Concrete, Lithium Oxide, Water, Blanket, Comparative Evaluations

---

* Century Research Center Corp., Tokyo, Japan

JAERI－M　82－054

核融合炉のブランケットと遮蔽材料の遮蔽性能の比較

日本原子力研究所東海研究所大型トカマク開発部
関　　泰・飯田　浩正・川崎　弘光*

（1982年5月12日受理）

核融合炉のブランケットと遮蔽材料の中で6種の候補材料の放射線遮蔽性能を比較した。6種の材料としてはかなり異なる核的性質を持ったもの，すなわち鉛，ステンレス鋼，重コンクリート，普通コンクリート，酸化リチウムと水を比較の対象とした。トカマク型核融合炉を単純化した計算モデルに上記材料を配置し，材料中の種々の核特性量やレスポンスの減衰を計算した。結果を図形表示して表の形にまとめて比較した。

比較した6種の材料の中では，14MeV中性子束の遮蔽にはステンレス鋼が，全中性子束の遮蔽には重コンクリートが，そしてガンマ線束の遮蔽には鉛が最も適していることが示された。

---

*　センチュリーリサーチセンター㈱

CONTENTS

目　　次

1. INTRODUCTION

In a D-T burning tokamak fusion reactor, radiation shield is an important component because it not only determines the overall size of the reactor but it also influences the repair and maintenance scheme. Since huge amount of the shielding materials will be required, the optimization of the shield thickness or cost becomes necessary. As the result, most of the optimized shield in recent design studies[(1)∿(3)] consist of multi-layered shield or mixture of several materials. It is rather difficult to estimate radiation attenuation characteristics of each material from such an optimized shield.

In this report, radiation shielding capabilities of six candidate materials are shown in a simplified model so that one may understand the mechanism of the interaction of 14 MeV neutron with each of the materials. The six materials with widely different nuclear characteristics, namely lead, stainless steel (SS-316), heavy concrete, ordinary concrete, lithium oxide (Li_2O) and water are chosen for the comparison. The result of the radiation shielding calculations presented in this report may be used to roughly estimate the required shield thickness of a fusion reactor.

In Section 2, the calculational model and method used for the comparison are described. The attenuation of various quantities of interest in terms of fusion reactor shielding is shown graphically in Section 3. In Section 4, the calculated results are summarized and compared in tables. Some discussions are given in the last Section.

2. CALCULATIONAL MODEL AND METHODS

A simplified model of a tokamak fusion reactor shown in Fig.1 is used for the comparison. The infinite cylinder model includes a 100 cm radius plasma surrounded by a shield material 100 cm thick. The D-T neutrons are uniformly generated in the plasma region. A 10 cm thick SS-316 annulus is placed behind the shield material to simulate the existence of the superconducting toroidal field coils for a real tokamak reactor. The six materials whose contents are given in Table I, are placed one by one in the shield material region and various nuclear characteristics and response values in the detector surface are calculated. The calculated items at the detector surface are the 14 MeV neutron flux, the flux of neutrons with energies greater than 0.1 MeV, the total neutron flux, the total gamma ray flux, heating rates, biological dose rates, displacement damage rates for the SS-316 and copper (Cu), and the reaction rates of the ^{58}Ni(n, p)^{58}Co and ^{58}Fe(n, γ)^{59}Fe reactions. The latter two reaction rates are important in relation to the induced activation of SS-316.

Using the same calculational model of Fig.1, the 1.25 MeV gamma rays are generated in the plasma region instead of D-T neutrons to investigate the shielding capabilities of the six materials for gamma rays from induced activation. The 1.25 MeV gamma ray is considered to be one of the most important and typical as a gamma ray source one day after shutdown in a fusion reactor [3].

The one-dimensional discrete ordinates transport code ANISN [4] is used with the P_5-S_8 approximation throughout the present study for the radiation transport calculations. The 42-group neutron and 21-group gamma ray coupled cross section set GICX40 [5] is used. This cross section set is based on the ENDF/B-III and IV nuclear data files(6) for neutron cross sections and on the POPOP4 Library(7) for gamma-ray production cross sections. For the processing, the RADHEAT code system(8) developed in JAERI was mainly used. The GAMLEG-JR code(9) was used to obtain gamma-ray transport cross sections and gamma-ray kerma factors. The MACK code(10) was used to obtain neutron kerma factors. The APPLE-2 code(11) was used to plot graphs shown in Section 3.

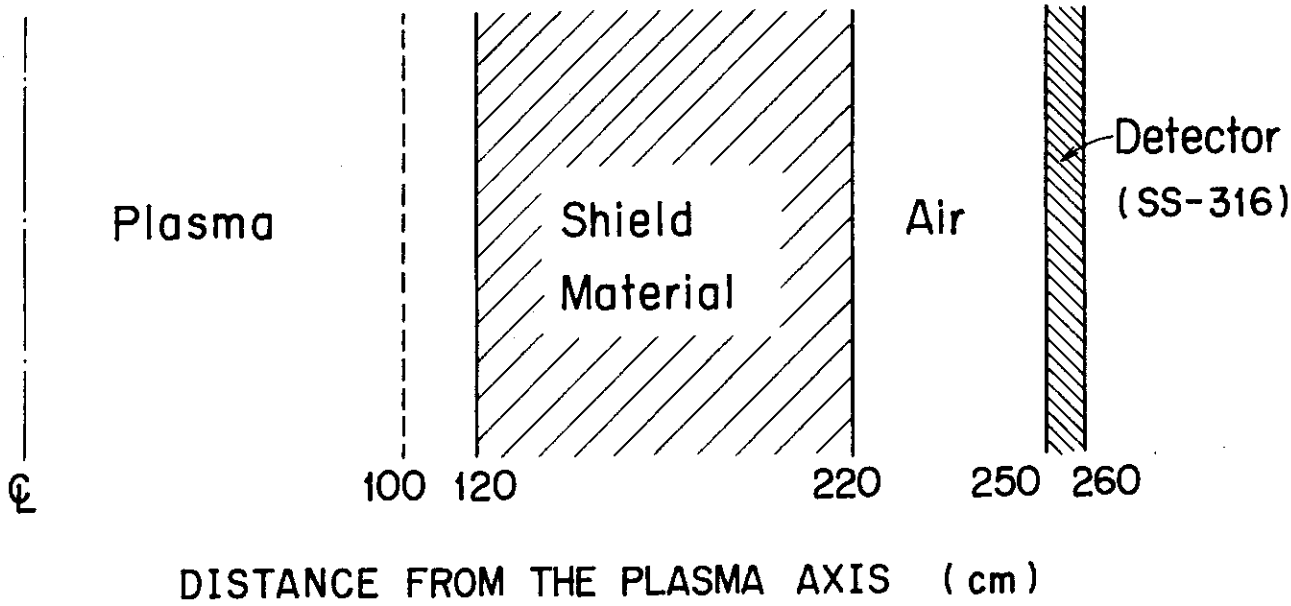

Fig. 1 Simplified Model of a Fusion Reactor

TABLE I NUCLIDE DENSITIES OF SIX MATERIALS

(atom/cm^3-barn)

Nuclide	Shield material					
	Lead	SS-316	Heavy Concrete	Ordinary Concrete	Li_2O	Water
H				1.40-2*		6.70-2
^6Li					5.12-3	
^7Li					6.39-2	
^{12}C				6.02-6		
^{16}O			3.39-2	4.57-2	3.45-2	3.35-2
Mg				5.63-4		
Al			3.03-3	3.29-3		
Si				1.44-2		
Ca			2.39-3	2.57-3		
Cr		1.58-2	6.30-3			
Fe		5.91-2	2.36-2	7.05-4		
Ni		9.85-3	3.94-3			
Mo		1.26-3	5.02-4			
Pb	3.30-2					

* read as 1.40×10^{-2}

3. CALCULATED RESULT DESCRIPTION

Calculated results for lead, stainless steel (SS-316), heavy concrete, ordinary concrete, lithium oxide (Li_2O) and water are shown in Figs. 2∿7, respectively.

Figs. 2a, 3a, ----, 7a show the calculated neutron spectra at the front surface of the shield materials facing the plasma (R = 120 cm), at the midpoint of the material (R = 170 cm) and at the surface of the detector (R = 250 cm). Figure 1 may serve to identify the corresponding positions more clearly. Neutron flux per unit lethargy ($n.\ cm^{-2}.\ S^{-1}.\ \Delta u^{-1}$) is plotted against the energy in logarithmic scale. Neutron flux value is normalized to unit source neutron.

Figs. 2b, 3b,---, 7b show the calculated secondary gamma ray spectra for each of the material in similar manner as the neutron spectra. Some of the values less than 10^{-20} in Figs. 2b and 3b are due to fictitious source values used to mitigate zero divide errors and are insignificant.

Figs. 2c, 3c,---, 7c represent the distribution of 14 MeV neutron flux, flux of neutrons with energies greater than 0.1 MeV, the total neutron flux and the total gamma ray flux in the calculational models. In Fig. 2c, the gamma ray from the detector is dominant at R = 220 cm.

Figs. 2d, 3d,---, 7d show the displacement damage rates and activation reaction rates. The damage rate is the displacement damage cross section in barn unit ($10^{-24}\ cm^{-2}$) convoluted with the neutron flux and represents the amount of displacement per atom (dpa) caused in stainless steel or copper sample if they are brought into the calculational model. Similarly, the activation reaction rates are the convolution of the cross section of the $^{58}Ni(n,p)^{58}Co$ reaction or $^{58}Fe(n,\gamma)^{59}Fe$ reaction and the neutron flux, i.e. $\int dE\ \sigma(E).\ \phi_n(E,\ r)$.

Figs. 2e, 3e,---, 7e show the nuclear heat deposition rate in ($MeV.\ cm^{-3}.\ S^{-1}$). Neutron heating rate, gamma ray heating rate and their sum are given separately.

Figs. 2f, 3f,---, 7f show the epoxy dose rate. The dose rate value is the amount absorbed in an epoxy sample per one year if the sample is brought to the position. Neutron dose rate, gamma ray dose rate and their total are given separately.

Figs. 2g, 3g, ---, 7g show the dose rate distribution when one 14 MeV source neutron is generated every second. Neutron dose rate, gamma dose rate and their sum are shown separately.

Figs. 2h, 3h,---, 7h show the dose rate distribution when one gamma ray (1.25 MeV) is generated every second. In Fig. 2h, the value smaller than 10^{-23} is influenced by the fictitious source input and should not be taken seriously.

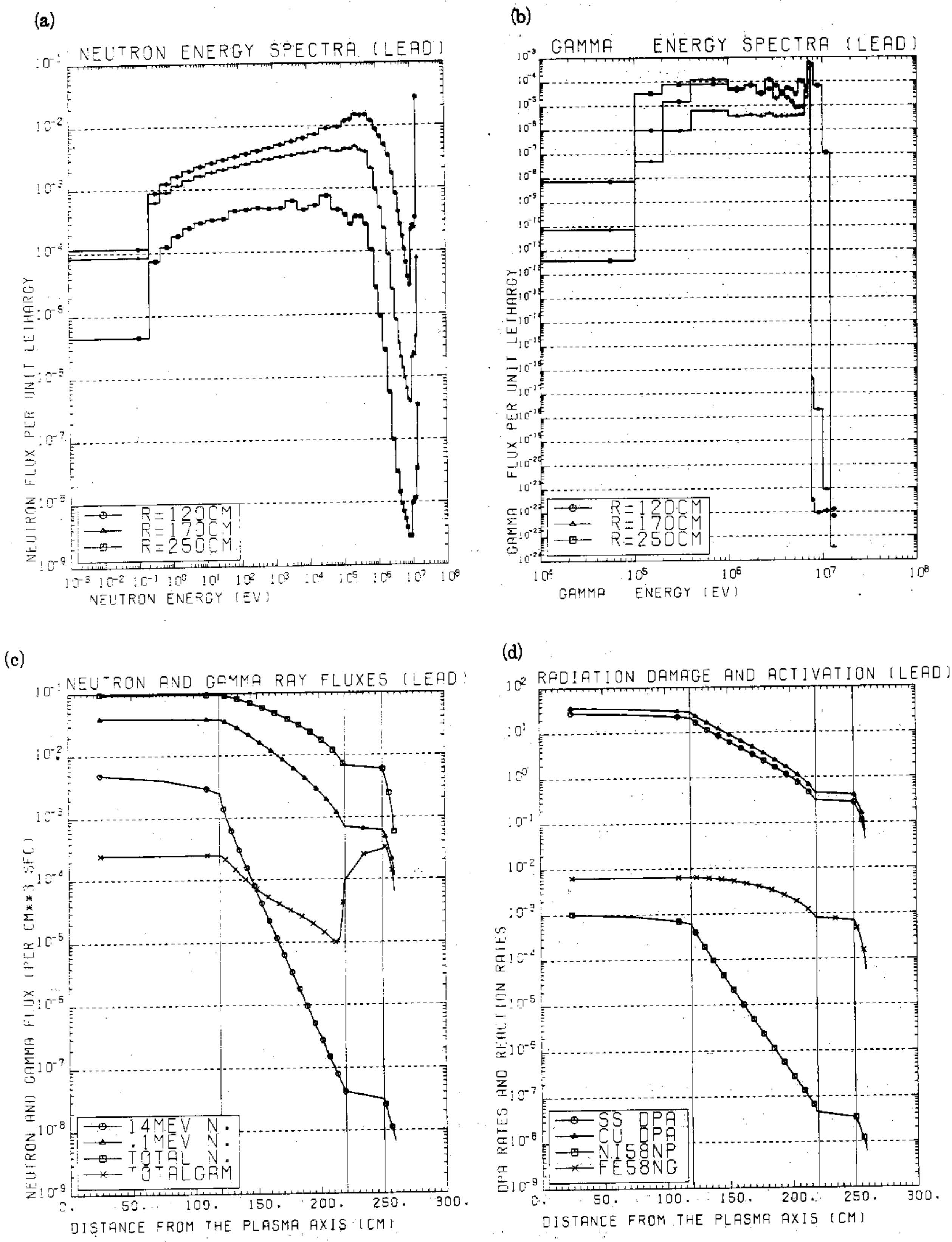

Fig. 2 Fusion Reactor Shielding Data for Lead

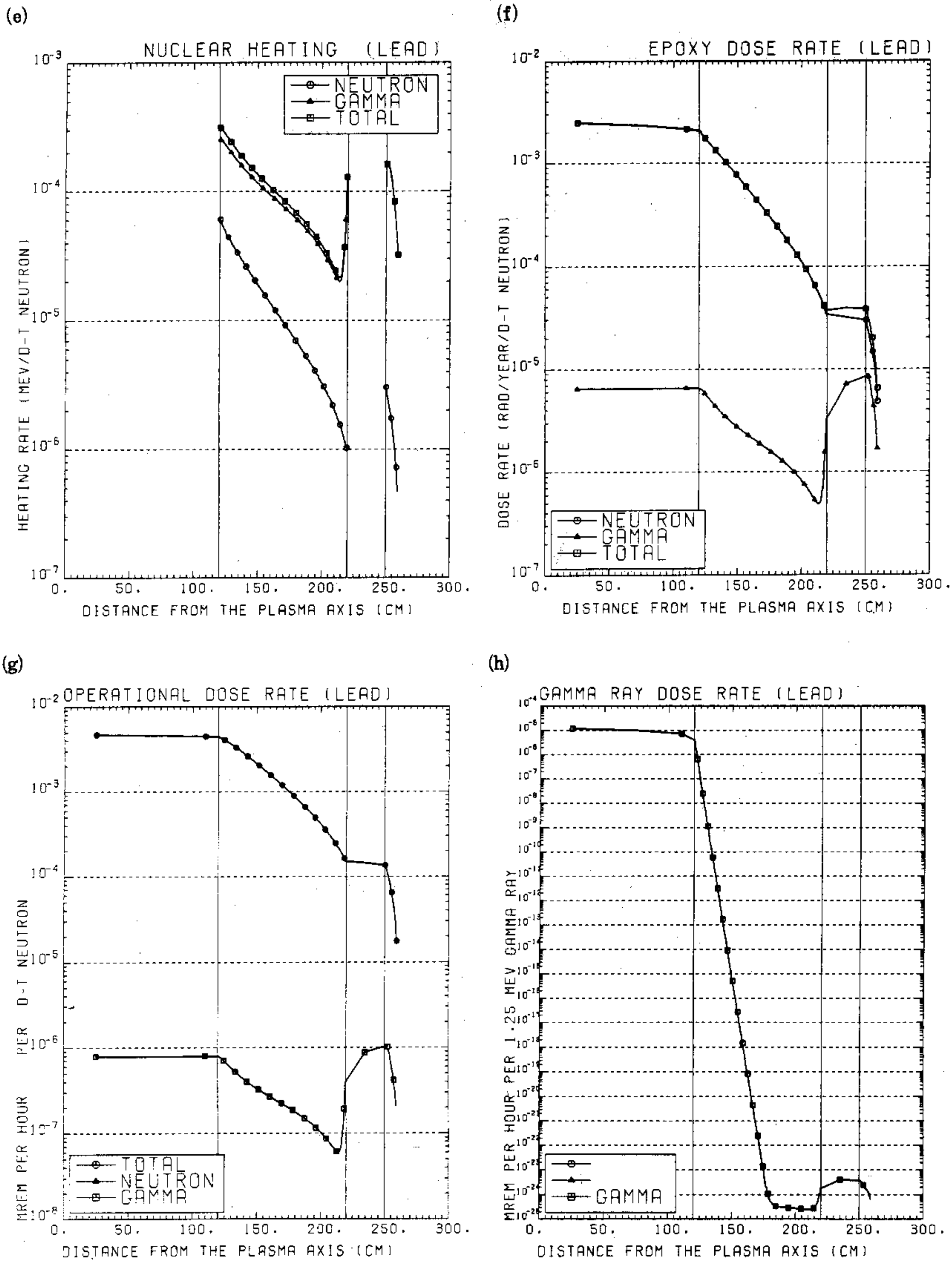

Fig. 2 continued

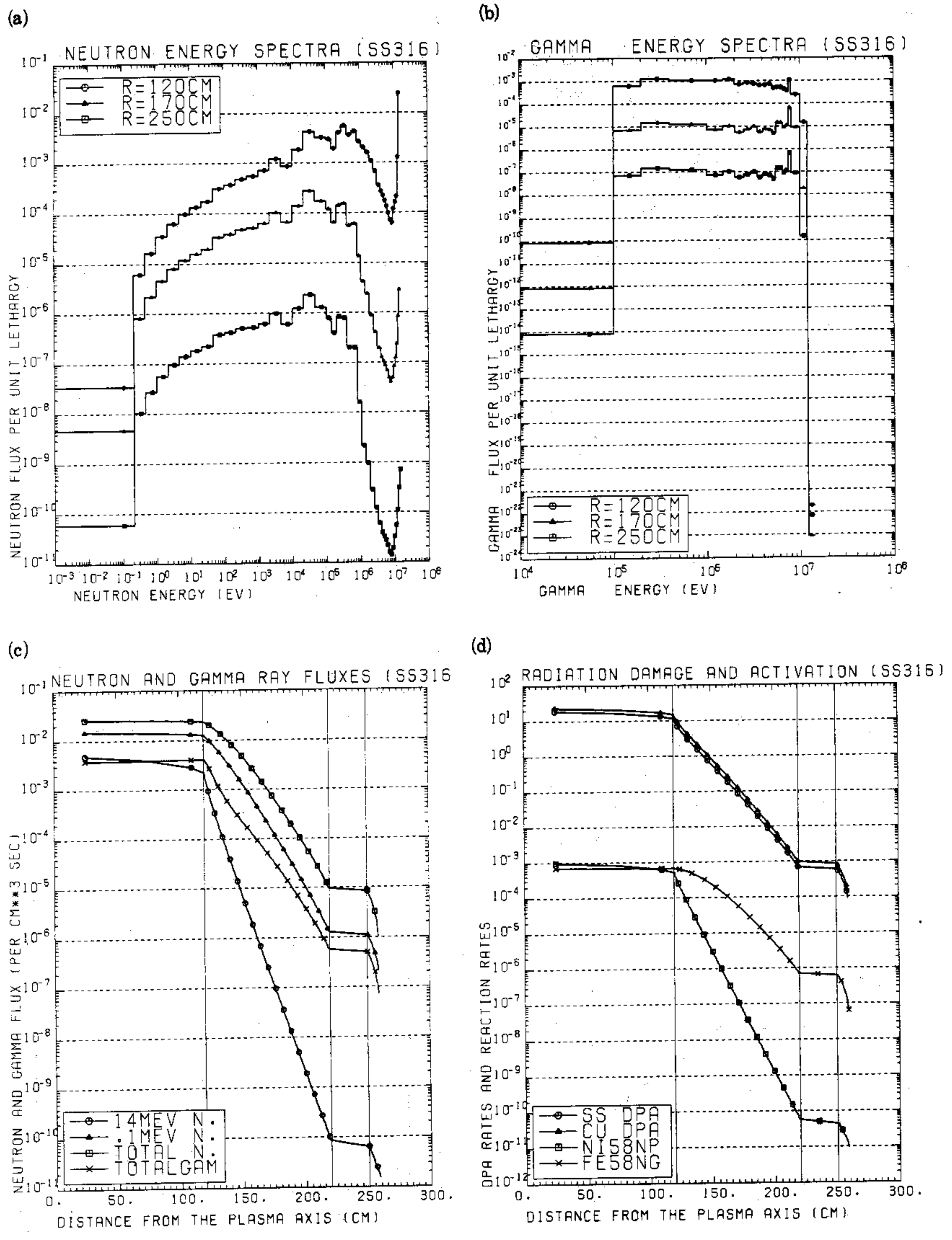

Fig. 3 Fusion Reactor Shielding Data for Stainless Steel (SS-316)

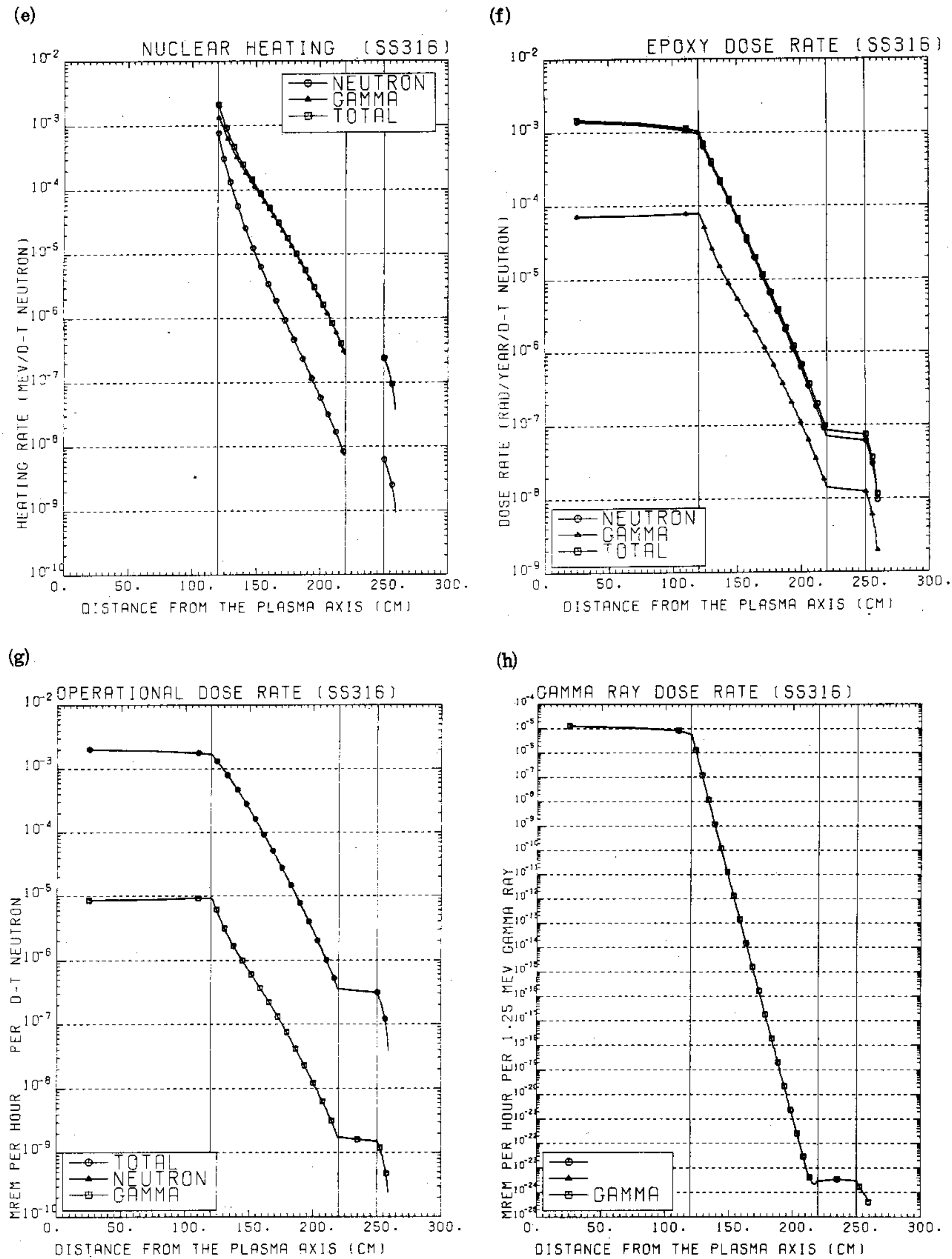

Fig. 3 continued

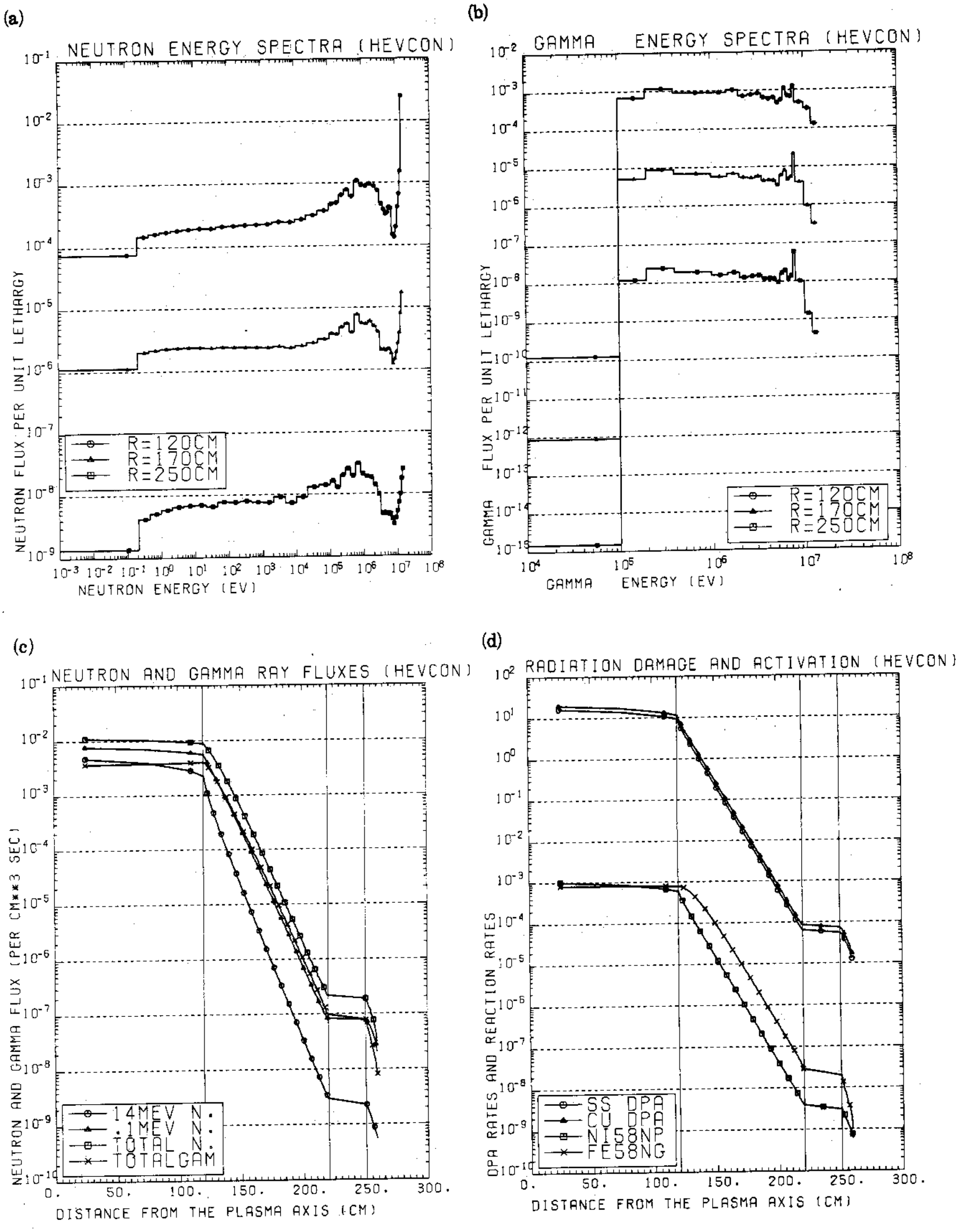

Fig. 4 Fusion Reactor Shielding Data for Heavy Concrete

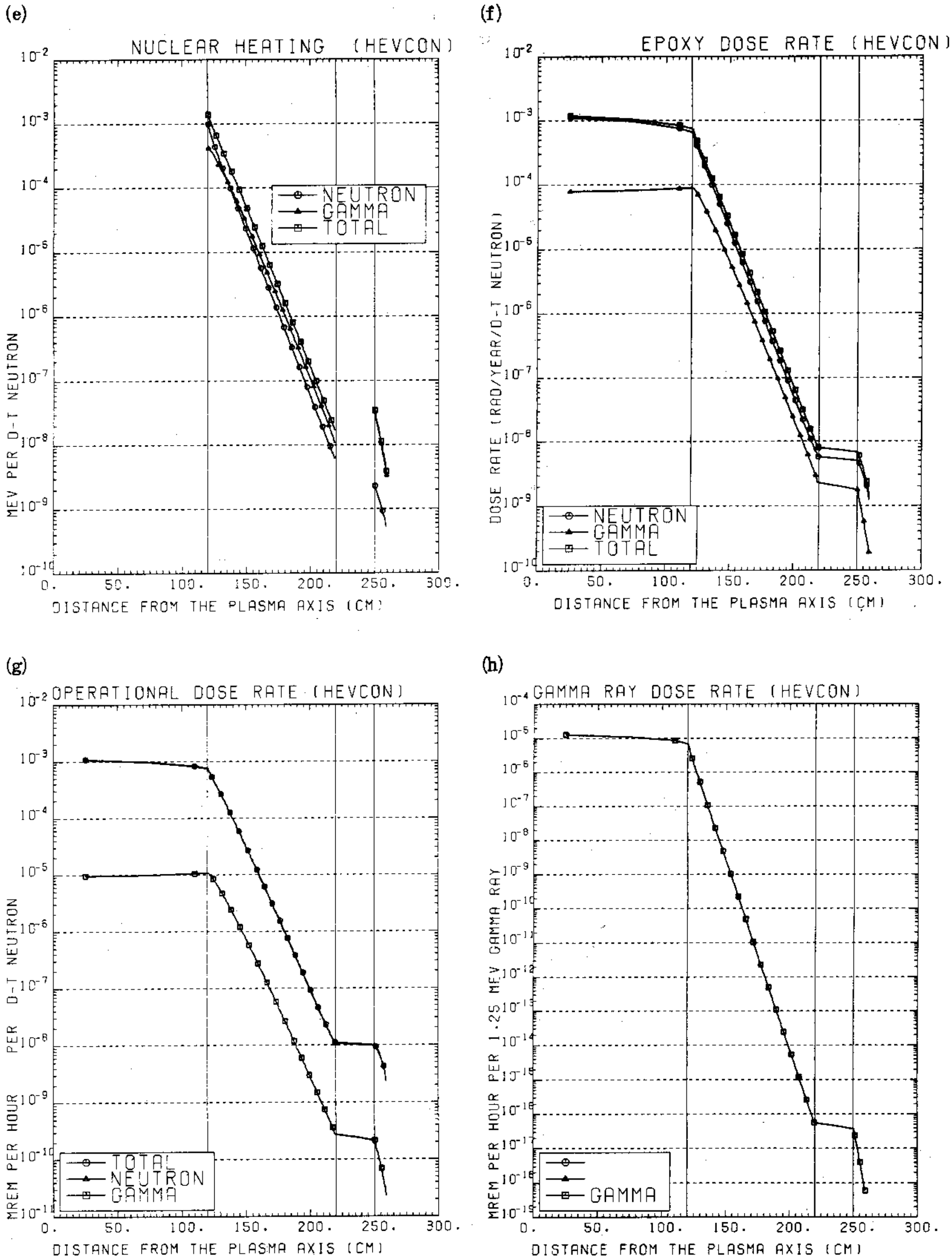

Fig. 4 continued

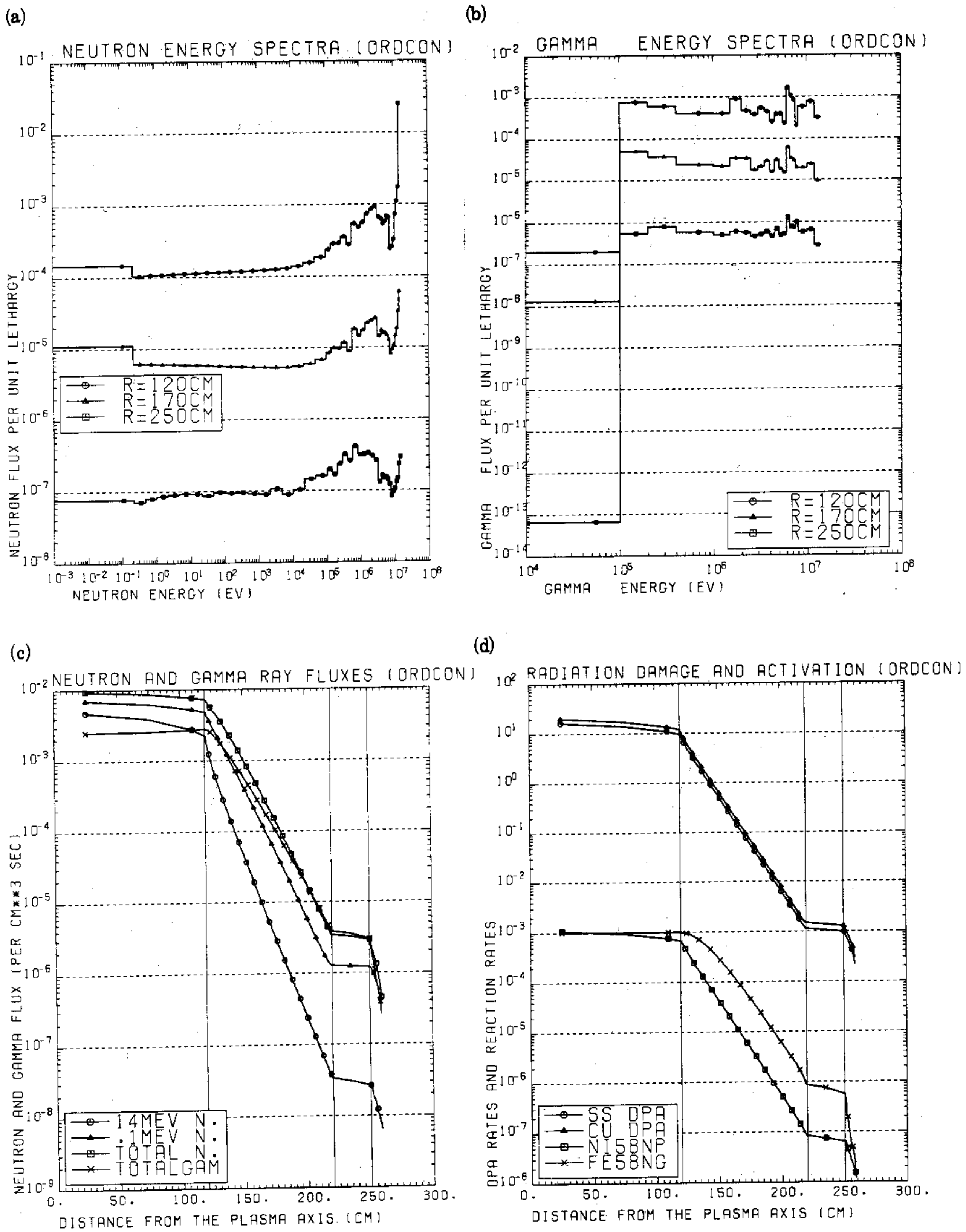

Fig. 5 Fusion Reactor Shielding Data for Ordinary Concrete

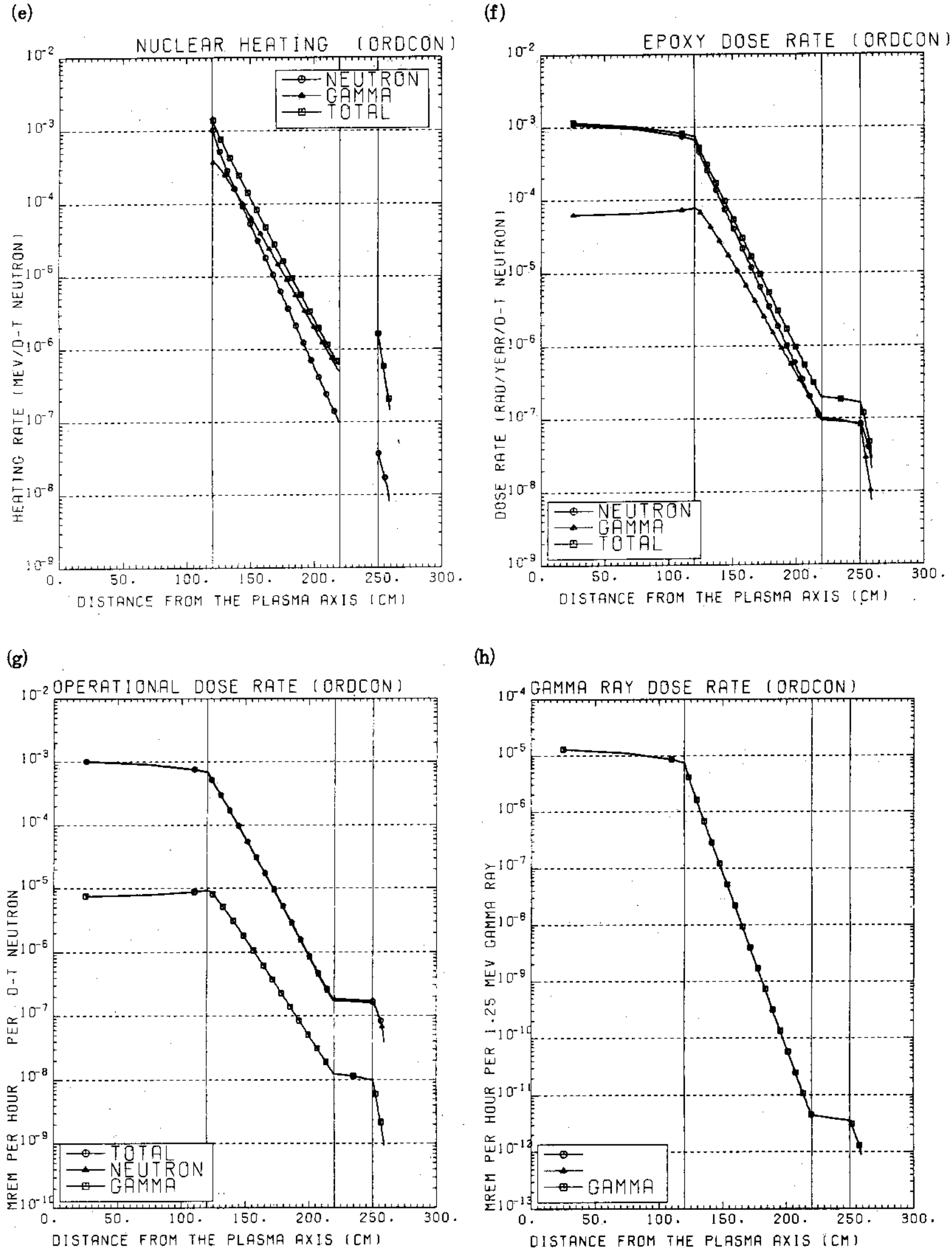

Fig. 5 continued

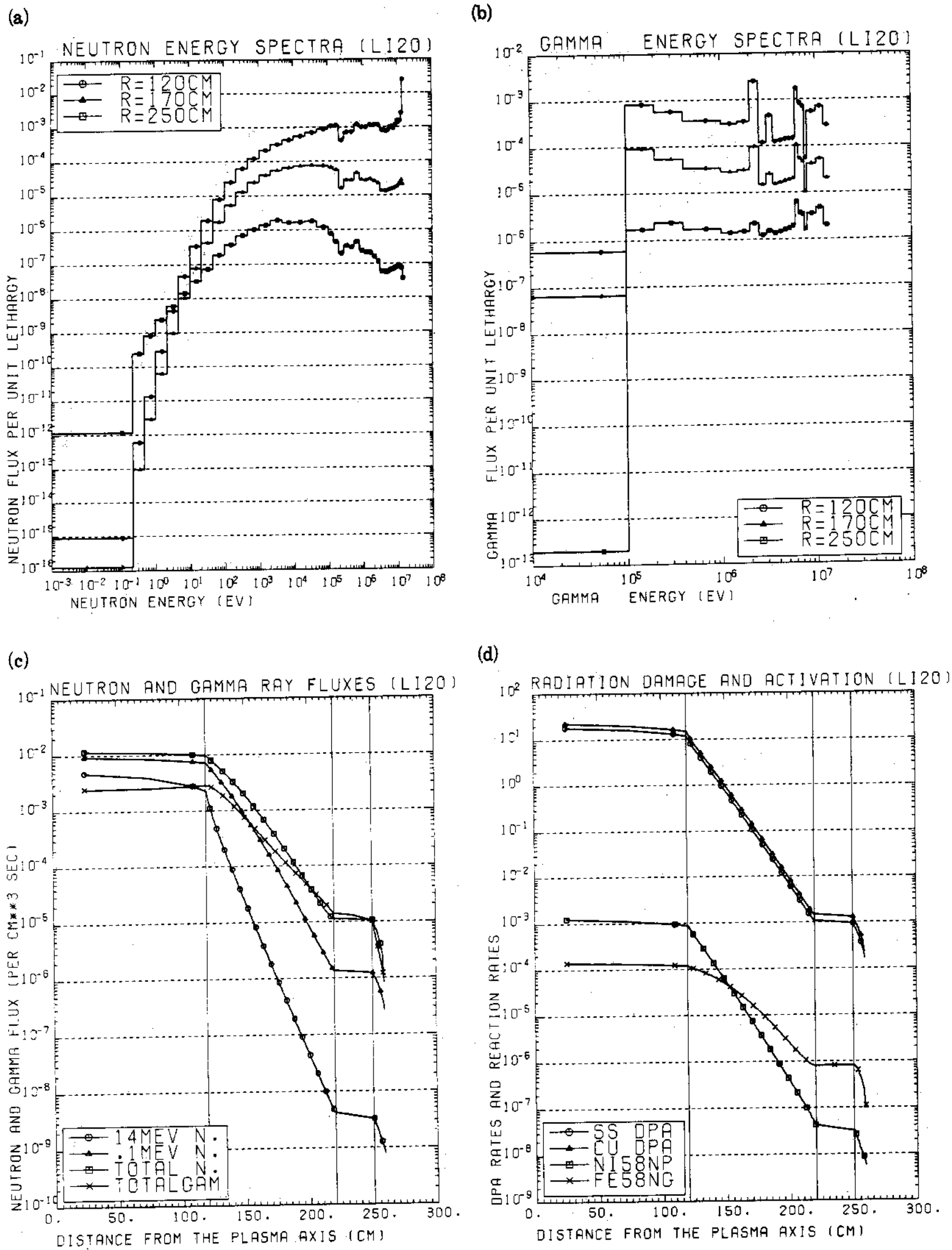

Fig. 6 Fusion Reactor Shielding Data for Lithium Oxide (Li_2O)

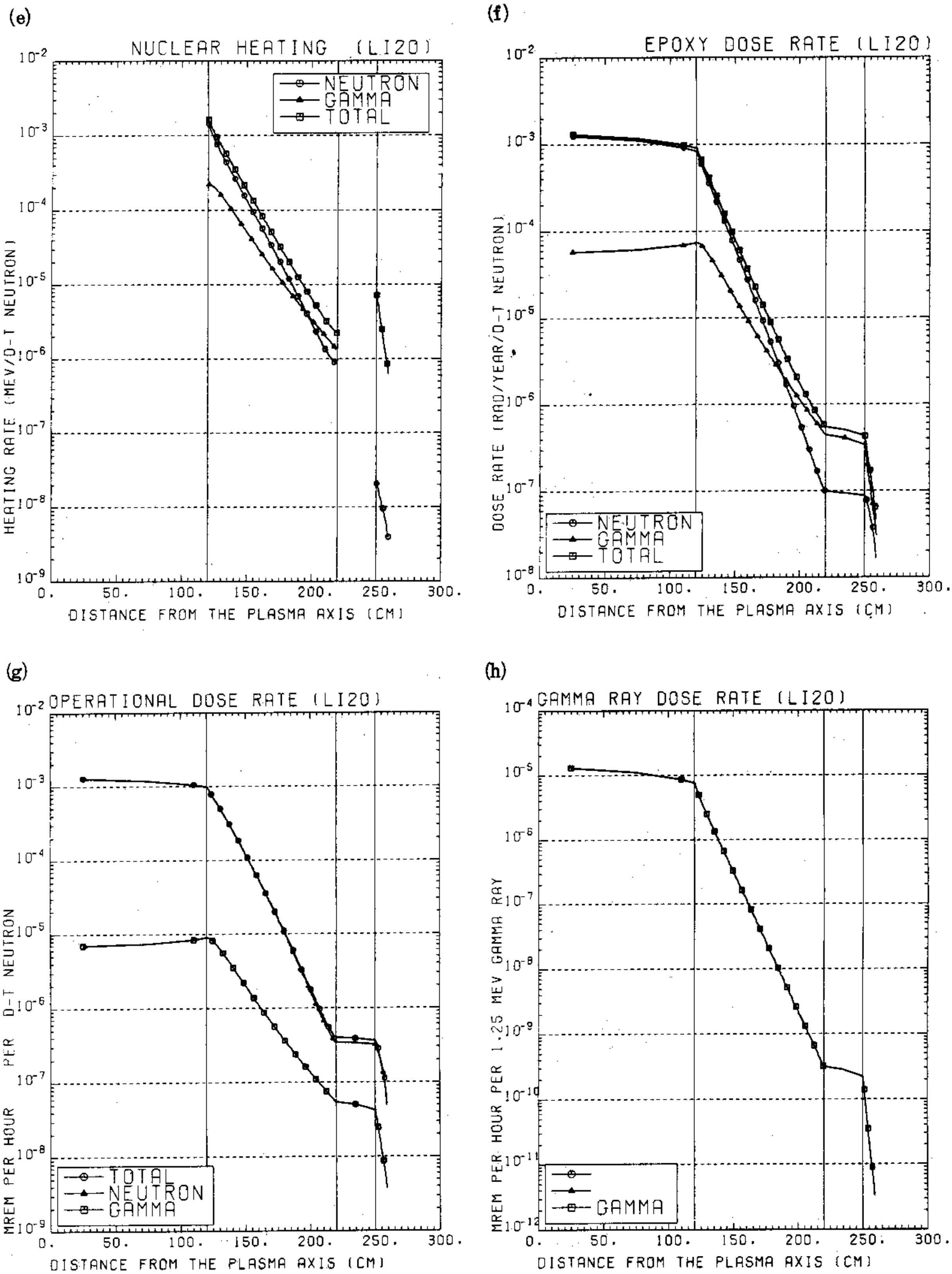

Fig. 6 continued

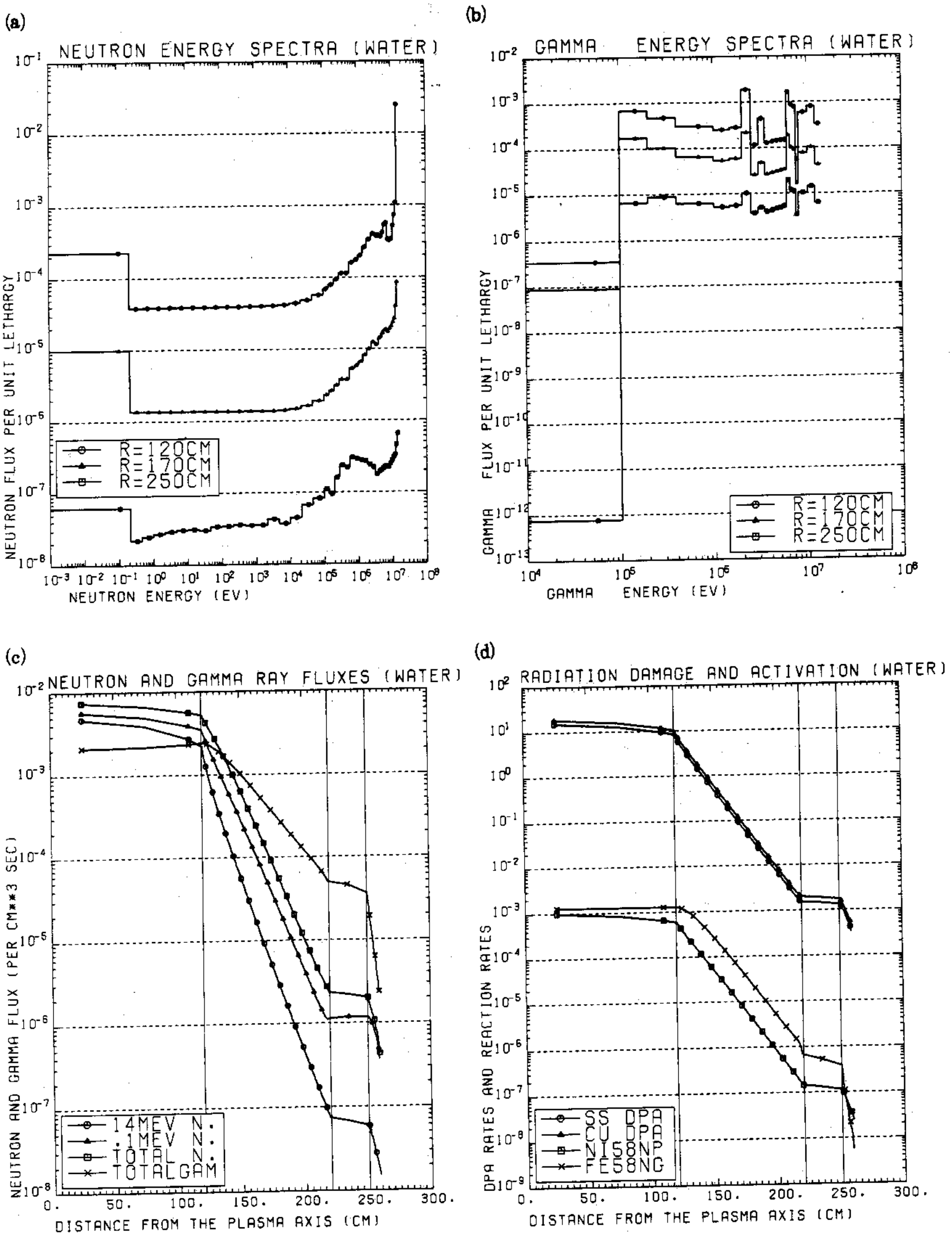

Fig. 7 Fusion Reactor Shielding Data for Water

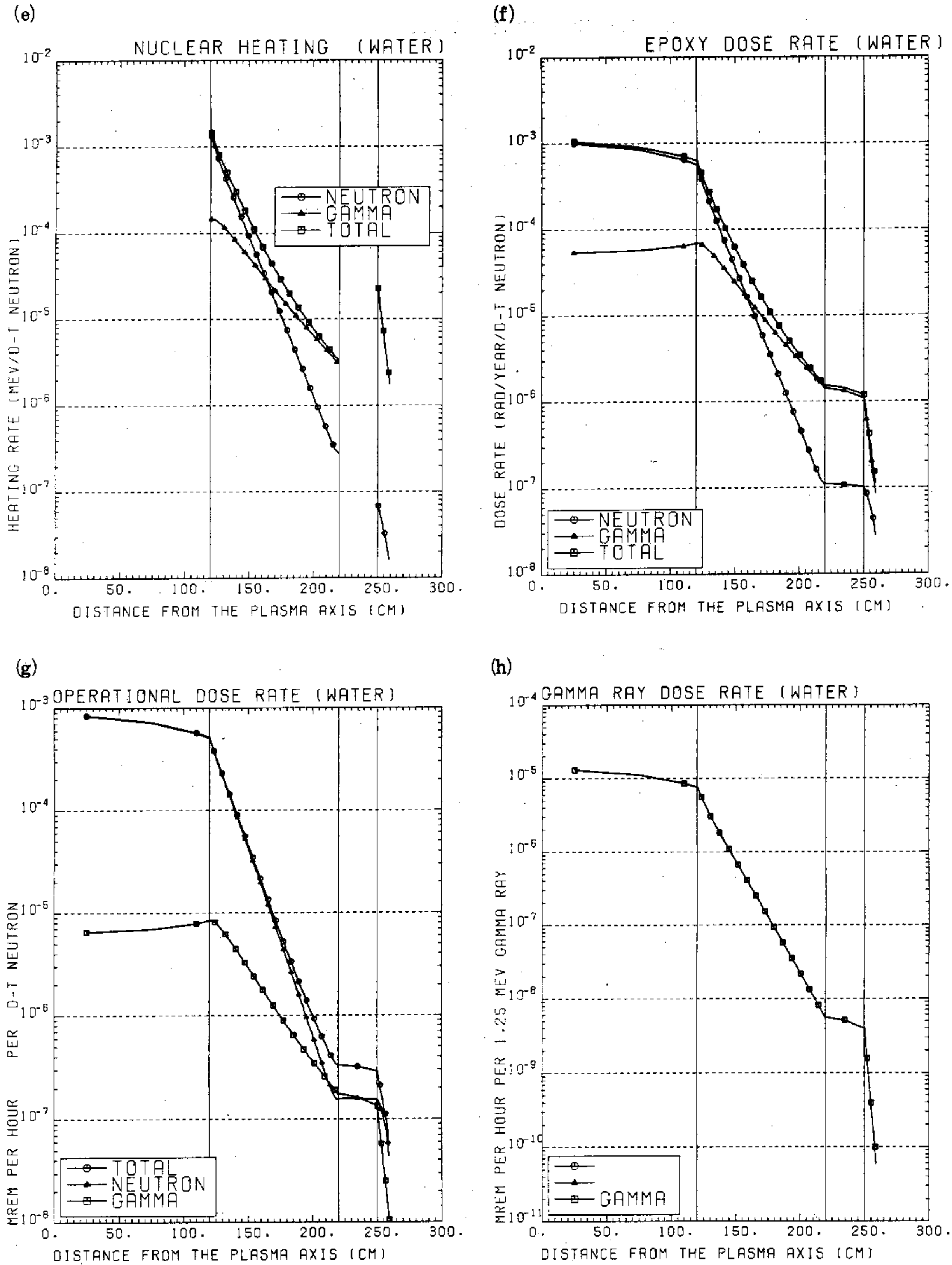

Fig. 7 continued

4. COMPARISON OF SHIELDING CAPABILITIES

Nuclear characteristic values at the stainless steel surface behind 1.0 m shield material are compared for the six shield materials in Table II. In the table all the values are normalized to unit neutron source. The maximum values and the minimum values among the six values for each item are depicted using straight overlines and waved underlines, respectively. Table II shows that the best shield material for reducing the 14 MeV neutron flux and the $^{58}Ni(n, p)^{58}Co$ reaction rate is SS-316 and the worst is water. It also shows that for reducing other quantities the heavy concrete is the best material and lead is the worst.

Table III compares the 1.25 MeV gamma flux, the total gamma flux, gamma heating rate, and gamma ray dose rate behind 50 cm thick shield materials. All the values are normalized to unit gamma ray source of 1.25 MeV. The gamma ray shielding capability is greater for materials with higher atomic numbers. Lead is the best material as a gamma shield and water is the worst.

Thickness values of materials required to reduce the 14 MeV neutron flux and the 1.25 MeV gamma-ray flux to one tenth in a slab geometry are given in Table IV. For the 1/10 reduction of the 14 MeV neutron flux, the required thickness ranges from 13.8 cm for SS-316 to 23.3 cm for water. In contrast, the required thickness for the 1/10 reduction of the 1.25 MeV gamma-ray flux varies over a wider range of 3.1 cm for lead to 34.1 cm for water.

TABLE II. NUCLEAR CHARACTERISTICS VALUES AT THE STAINLESS STEEL SURFACE BEHIND 1.0M SHIELD MATERIAL FOR A UNIT D-T NEUTRON SOURCE

Item	Shield material					
	Lead	SS-316	Heavy concrete	Ordinary concrete	Li_2O	Water
14 MeV neutron flux ($n \cdot cm^{-2} \cdot s^{-1}$)	3.10-8*	6.36-11	2.26-9	2.65-8	3.24-9	5.86-8
E_n > 0.1 MeV neutron flux ($n \cdot cm^{-2} \cdot s^{-1}$)	6.13-4	1.11-6	7.76-8	1.21-6	1.27-6	1.17-6
Total neutron flux ($n \cdot cm^{-2} \cdot s^{-1}$)	5.90-3	8.38-6	1.87-7	2.90-6	1.04-5	2.00-6
Total gamma ray flux ($\gamma \cdot cm^{-2} \cdot s^{-1}$)	3.06-4	5.00-7	7.80-8	2.98-6	1.03-5	3.56-5
Neutron heating ($MeV \cdot cm^{-3} \cdot s^{-1}$)	3.02-6	6.25-9	2.28-9	3.68-8	2.08-8	6.80-8
Gamma heating ($MeV \cdot cm^{-3} \cdot s^{-1}$)	1.59-4	2.33-7	3.22-8	1.58-6	7.12-6	2.24-5
Total heating ($MeV \cdot cm^{-3} \cdot s^{-1}$)	1.62-4	2.39-7	3.45-8	1.62-6	7.14-6	2.24-5
Neutron dose (mrem/hr)	1.36-4	3.10-7	9.86-9	1.58-7	3.20-7	1.54-7
Gamma dose (mrem/hr)	1.03-6	1.51-9	2.14-10	9.84-9	4.19-8	1.33-7
Total dose (mrem/hr)	1.37-4	3.11-7	1.01-8	1.68-7	3.62-7	2.87-7
SS dpa ($10^{-24} \cdot cm^{-2} \cdot s^{-1}$)	2.79-1	5.90-4	5.48-5	9.67-4	9.30-4	1.32-3
Cu dpa ($10^{-24} \cdot cm^{-2} \cdot s^{-1}$)	4.07-1	8.41-4	7.33-5	1.27-3	1.29-3	1.73-3
$^{58}Ni(n,p)^{58}Co$ ($reactions \cdot cm^{-3} \cdot s^{-1}$)	3.42-8	4.40-11	2.99-9	6.43-8	3.14-8	1.14-7
$^{58}Fe(n,\gamma)^{59}Fe$ ($reactions \cdot cm^{-3} \cdot s^{-1}$)	6.97-4	6.17-7	1.98-8	5.61-7	8.09-7	3.83-7

* read as 3.10×10^{-8}

~~~~ the minimum values

—— the maximum values
~~~~

TABLE III. NUCLEAR CHARACTERISTICS VALUES BEHIND 50 CM SHIELD MATERIAL FOR A UNIT 1.25 MeV GAMMA-RAY SOURCE

Item	Shield material					
	Lead	SS-316	Heavy concrete	Ordinary concrete	Li_2O	Water
1.25 MeV gamma-ray flux ($\gamma \cdot cm^{-2} \cdot s^{-1}$)	8.46-20*	1.10-13	2.20-9	6.96-7	6.40-6	2.96-5
Total gamma-ray flux ($\gamma \cdot cm^{-2} \cdot s^{-1}$)	1.20-19	5.02-13	1.13-8	5.43-6	5.35-5	2.18-4
Gamma heating in the shield material ($MeV \cdot cm^{-3} \cdot s^{-1}$)	6.58-20	8.88-14	1.05-9	2.02-7	1.25-6	3.66-6
Gamma ray dose (mrem/hr)	2.52-22	6.40-16	1.34-11	4.57-9	4.10-8	1.75-7

* read as 8.46×10^{-20}

~~~ the minimum values

——— the maximum values

TABLE IV. THICKNESS OF MATERIALS REQUIRED TO REDUCE TO ONE TENTH THE FLUXES OF 14 MEV NEUTRONS AND 1.25 MEV GAMMA RAYS

(cm)

Item	Shield materials					
	Lead	SS-316	Heavy concrete	Ordinary concrete	Li_2O	Water
14 MeV neutron flux	21.9	13.8	17.5	21.5	18.0	23.3
1.25 MeV gamma-ray flux	3.1	5.1	9.0	16.4	23.9	34.1
~~~

5. DISCUSSIONS

The neutron spectra for the six materials in Figs. 2a, 3a,---, 7a show quite distinctly the nuclear characteristics of each material. Fig. 2a shows the low capability of lead in shielding neutron. Strong neutron moderating capability of hydrogen is most apparent in water (Fig. 7a). The hydrogen also strongly influences the neutron spectra in ordinary concrete and heavy concrete (Figs. 4a and 5a). The neutron absorption of ^{6}Li is distinct in Li_2O spectra in Fig. 6a.

The gamma ray spectra in Figs. 2b, 3b,---, 7b are more similar for the six materials than the neutron spectra. The gamma ray spectra for Li_2O and H_2O are very much alike both dominated by oxygen gamma rays.

From Table II, among the six shield materials, stainless steel is shown to be the best material for attenuating the 14 MeV neutron flux and the activation reaction rates dominated by 14 MeV neutron flux e.g. $^{58}Ni(n. p)^{58}Co$. The poorest material for the attenuation of the 14 MeV neutron flux is water but the thickness required to reduce the 14 MeV neutron flux to 1/10 is only 70 % more than stainless steel as shown in Table IV.

Heavy concrete is the best material for reducing the total neutron flux and most of the quantities of interest in fusion reactor shielding. Water is the second best material for reducing the total neutron flux. These facts suggest proper mixture of stainless steel and other lighter element is effective for the fusion reactor shielding.

Gamma ray shielding capability is proportional to the electron density in the material. Thus lead is the best and water the worst. As shown in Table III, the one tenth reduction thickness of 1.25 MeV gamma ray differs as much as 10 times between lead and water. In order to compensate the poor gamma-ray shielding capability of water, the use of some heavy element material in combination with water is recommended to achieve effective shielding.

It is hoped that the results presented in this report will be utilized to obtain rough estimate values of the required shield thickness in fusion reactors.

REFERENCES

(1) B.A. Engholm, "Preliminary Radiation Criteria and Nuclear Analysis for ETF," GA-A16072, General Atomic Company (1980)

(2) M.A. Abdou, Y. Gohar, and J. Jung, "Radiation Shielding," INTOR/NUC/81-10, USA Conceptual Design Contribution to the INTOR Phase-1 Workshop, March (1981)

(3) Y. Seki, H. Iida and H. Kawasaki, "Fusion Reactor Shield Optimization in Terms of Personnel Access," J. Nucl. Sci. Technol., 19[1], 11 (1982)

(4) W.W. ENGLE,,Jr., "A Users Manual for ANISN, a One-Dimensional Discrete Ordinates Transport Code with Anisotropic Scattering," Computing Technology Center, Union Carbide Corporation, K-1693(1976)

(5) Y. SEKI, H. IIDA, "Coupled 42-Group Neutron and 21-Group Gamma Ray Cross Section Set for Fusion Reactor Calculations, "Japan Atomic Energy Research Institute Rep. JAERI-M 8818(1980)

(6) M.K. Drake (edited), "Data Formats and Procedures for the ENDF Neutron Cross Section Library," BNL-50274 (T-601, TID-4500), ENDF 102, Vol. 1 (1970), Revised 1974

(7) W.E. Ford, III, "The POPOP4 Library of Neutron-Induced Secondary Gamma-Ray Yield and Cross-Section Data," CTC-42, UCC-ND (1970)

(8) S. Miyasaka, et al., "Code System for the Radiation-Heating Analysis of a Nuclear Reactor, RADHEAT," JAERI-M 5794 (1974) in Japanese

(9) S. Miyasaka, et al., "GAMLEG-JR, A Production Code of Multigroup Cross Sections and Energy Deposition Coefficients of Gamma-Rays," JAERI-M 6936 (1977)

(10) M.A. Abdou, C.W. Maynard and R.Q. Wright, "MACK — A Computer Program to Calculate Neutron Energy Release Parameters (Fluence-to Kerma Factors) and Multigroup Neutron Reaction Cross Sections from Nuclear Data in ENDF Format," ORNL/TM-3994 (July 1973)

(11) H. Kawasaki and Y. Seki, "APPLE-2: An Improved Version of APPLE Code for Plotting Neutron and Gamma Ray Spectra and Reaction Rates," to be published as JAERI-M Report.